AFRL-ML-WP-TR-1999-4014

COMPOSITE MATERIALS FOR ADVANCED GLOBAL MOBILITY CONCEPTS

D.P ANDERSON
A.K. ROY

UNIVERSITY OF DAYTON RESEARCH INSTITUTE
300 COLLEGE PARK AVENUE
DAYTON, OH 45469-0168

DECEMBER 1998

INTERIM REPORT FOR 09/15/1997 – 09/14/1998

APPROVED FOR PUBLIC RELEASE; DISTRIBUTION UNLIMITED

MATERIALS AND MANUFACUTURING DIRECTORATE
AIR FORCE RESEARCH LABORATORY
AIR FORCE MATERIEL COMMAND
WRIGHT-PATTERSON AIR FORCE BASE OH 45433-7734

NOTICE

Using Government drawings, specifications, or other data included in this document for any purpose other than Government procurement does not in any way obligate the U.S. Government. The fact that the Government formulated or supplied the drawings, specifications, or other data does not license the holder or any other person or corporation; or convey any rights or permission to manufacture, use, or sell any patented invention that may relate to them.

This report is releasable to the National Technical Information Service (NTIS). At NTIS, it will be available to the general public, including foreign nations.

This technical report has been reviewed and is approved for publication.

JAMES R. McCOY, Research Chemist
Composites Team
Structural Materials Branch

L. SCOTT THEIBERT, Chief
Structural Materials Branch
Nonmetallic Materials Division

ROGER D. GRISWOLD, Assistant Chief
Nonmetallic Materials Division
Materials and Manufacturing Directorate

Do not return copies of this report unless contractual obligations or notice on a specific document requires its return.

REPORT DOCUMENTATION PAGE

Form Approved
OMB No. 0704-0188

1. AGENCY USE ONLY *(Leave blank)*	2. REPORT DATE	3. REPORT TYPE AND DATES COVERED
	DECEMBER 1998	INTERIM REPORT FOR 09/15/1997 - 09/14/1998

4. TITLE AND SUBTITLE
COMPOSITE MATERIALS FOR ADVANCED GLOBAL MOBILITY CONCEPTS

5. FUNDING NUMBERS
C F33615-95-D-5029
PE 61102
PR 4347
TA 34
WU 10

6. AUTHOR(S)
D.P. ANDERSON
A.K. ROY

7. PERFORMING ORGANIZATION NAME(S) AND ADDRESS(ES)
UNIVERSITY OF DAYTON RESEARCH INSTITUTE
300 COLLEGE PARK AVENUE
DAYTON, OH 45469-0168

8. PERFORMING ORGANIZATION REPORT NUMBER
UDR-TR-98-000147

9. SPONSORING/MONITORING AGENCY NAME(S) AND ADDRESS(ES)
MATERIALS AND MANUFACTURING DIRECTORATE
AIR FORCE RESEARCH LABORATORY
AIR FORCE MATERIEL COMMAND
WRIGHT-PATTERSON AFB, OH 45433- 7734
POC: JAMES R. McCOY, AFRL/MLBC, 937-255-9063

10. SPONSORING/MONITORING AGENCY REPORT NUMBER
AFRL-ML-WP-TR-1999-4014

11. SUPPLEMENTARY NOTES

12a. DISTRIBUTION AVAILABILITY STATEMENT
APPROVED FOR PUBLIC RELEASE, DISTRIBUTION UNLIMITED

12b. DISTRIBUTION CODE

13. ABSTRACT *(Maximum 200 words)*

A variety of techniques were modified, adapted, or reconstituted to measure properties of graphitic foams. Successful measurements of tensile and shear mechanical properties, foam cell sizes, graphitic crystalline parameters, and foam deformation mechanisms were demonstrated. Thermal diffusivity measurements were close to being demonstrated, compression testing was found to be not reliable.

14. SUBJECT TERMS
bubble sizes, crystalline parameters, deformation mechanism, foam, graphitic foam, mechanical testing, shear properties, tensile properties, thermal diffusivity.

15. NUMBER OF PAGES
27

16. PRICE CODE

17. SECURITY CLASSIFICATION OF REPORT	18. SECURITY CLASSIFICATION OF THIS PAGE	19. SECURITY CLASSIFICATION OF ABSTRACT	20. LIMITATION OF ABSTRACT
UNCLASSIFIED	UNCLASSIFIED	UNCLASSIFIED	SAR

CONTENTS

FIGURES

FIGURES (Concluded)

TABLES

FOREWORD

This report was prepared by the University of Dayton Research Institute under Air Force Contract No. F33615-95-D-5029, Delivery Order No. 0006. The work was administered under the direction of the Nonmetallic Materials Division, Materials and Manufacturing Directorate, Air Force Research Laboratory, Air Force Materiel Command, with Dr. James R. McCoy (AFRL/MLBC) as Project Engineer.

This report was submitted in January 1999 and covers work conducted from 15 September 1997 through 14 September 1998.

EXECUTIVE SUMMARY

Graphitic foams have been produced that may find uses in a variety of applications from honeycomb core replacement to 3-D isotropic reinforcement. In order to use these materials in some of these applications, different properties need to be measured for design and analysis. The measurement of these properties in foams is not the same as in composites or conventional foam measurements. This task was then focused on developing and adapting the currently used measurement techniques for use on the brittle graphitic foams.

The mechanical property tests evaluated were compression, tension, and shear strength and moduli. Compression testing failed in these materials due to localized buckling at the fixture interface. Tension was accomplished by tabbing the material in order to obtain good load transfer. Dog-boning the samples was shown to be viable but unnecessary. Shear measurements were made using a newly constructed cylindrical torsion device. Good comparisons resulted between the tensile properties measured and those predicted from the shear results.

Microstructural properties of the foams were measured using optical microscopy and image analysis to obtain cell sizes after suitably modifying standard methods. Crystalline parameters were measured after control software was updated, installed, and debugged on the x-ray diffractometer. The basic measurement apparatus for thermal diffusivity was set up and tested; certain modifications still need to be made to measure this property on foams. An *in situ* load cell was tested in an electron microscope to observe the deformation mechanisms of the foams. Ligament juncture angle changes appear to be more dominant than ligament deformation. Limited depth-of-field precluded the use of optical microscopy of these measurements.

1. EXPERIMENTAL METHODS FOR MEASURING TENSILE AND SHEAR STIFFNESS AND STRENGTH OF GRAPHITIC FOAM

Microcellular graphitic foam is emerging as an ultralightweight material for many structural applications, such as core materials for a sandwich structure, net shape fabrication of structural components reinforced with fiber preforms, etc. This material macroscopically possesses isotropic properties, which is an added advantage over that of traditional honeycomb materials. The micrograph of a graphitic (open-cell) foam microstructure is shown in Figure 1. A representative unit of an open-cell foam, based on the minimum surface energy during the foaming process (i.e., the bubble nucleation process), possesses a tetrahedral structure of the foam ligaments oriented approximately 109° with each other (see Figure 2). Due to the tetrahedral cell microstructure, the macroscopic properties, such as foam modulus and strength, are critically influenced by the deformation characteristics of the cell ligaments. Thus, in order to develop a basic understanding of the performance of open-cell foam materials, the deformation and failure mechanism of the cell ligaments, critically needs to be studied.

The long-term objective of this work is to understand the deformation characteristics of cell ligaments subjected to external loading and correlate the ligament properties with the processing parameters. An appropriate mechanics model will be used to correlate the ligament properties to the foam bulk (macroscopic) properties to address the long-term objective. As an initial step towards the long-term objective, the goal for the present study is to develop suitable test methods to measure the bulk (macroscopic) mechanical properties of open-cell foam materials. Due to the open porosity of this material, the standard test methods

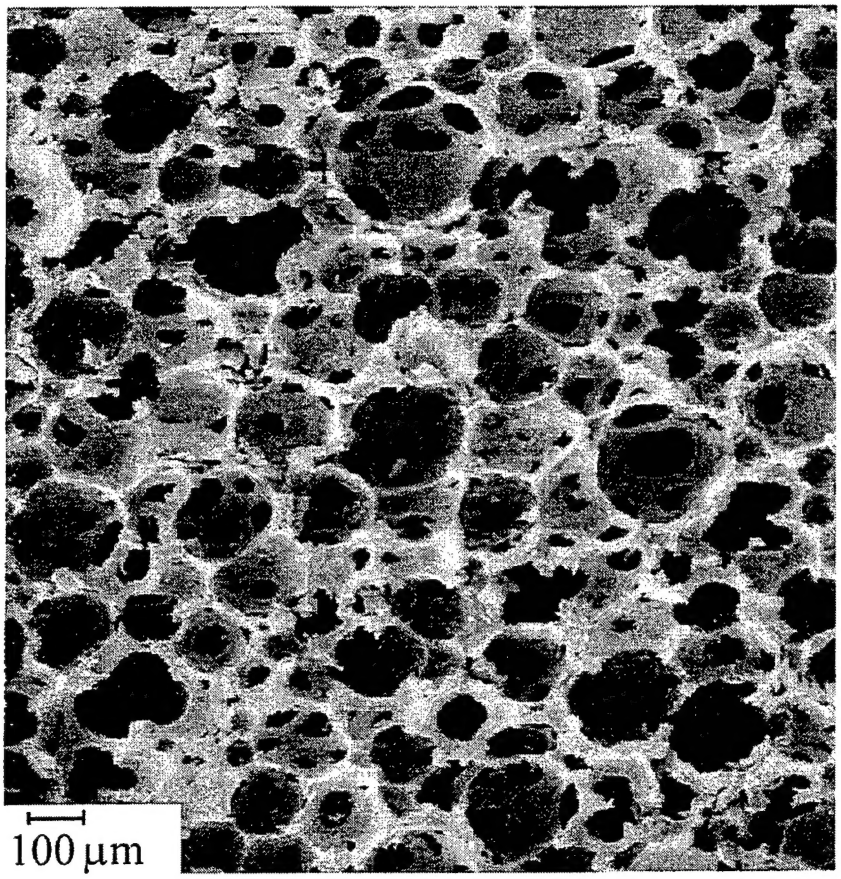

Figure 1. A Representative Microstructure of a Graphitic Foam.

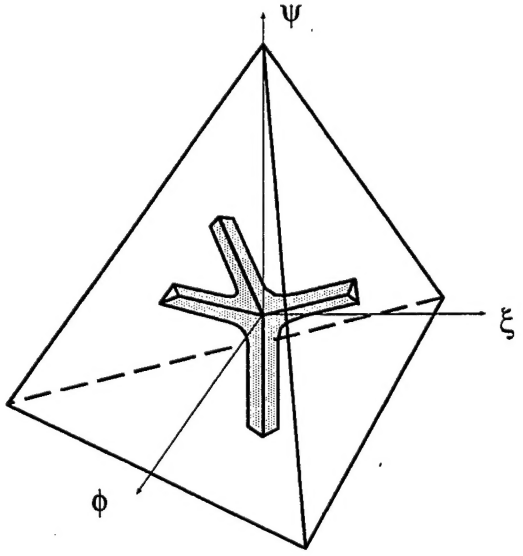

Figure 2. A Tetrahedral Representative Volume Element (RVE) of a Foam Microstructure. The axes of the four ligaments in the RVE are oriented normal to the respective tetrahedral surfaces.

that are used to measure properties of nonporous materials are not appropriate for measuring the stiffness and strength of foam materials of large porosity (e.g., 80 percent or higher).

1.1 Test Methods

A new generation of graphitic foam (porous) materials is being developed *[1-4]* with its intended use in structural components as load-carrying members. Thus there is a need for developing test methods to characterize the mechanical properties (stiffness and strength) of this material for various loading conditions, such as compression, tension, and shear. Traditionally, due to ease of loading and its intended use in the past, porous (foam) materials have been generally characterized in compression. As an illustration, the compressive stress-strain behavior of a carbonized phenolic foam with 82 percent porosity is shown in Figure 3. A one-inch cube of the material was subjected to block compression in this case. The initial small slope (up to one percent of the strain) in this stress-stain curve is attributed to excessive deformation of the cell ligaments exposed to the surface. The material appears to carry load up to a strain level of two percent; beyond that strain level the material fails to carry any further loading, as revealed in the stress-strain curve. The same material, however, in tensile loading appears to carry a load much more than two percent of tensile strain. The apparent failure of the material in compression at about two percent of the strain is attributed to the buckling failure of the cell ligaments. Thus, the cell ligaments are not loaded to its true load-carrying capability if the foam is loaded in compression. One of the objectives of this study is to correlate the effects of the processing parameters on the ligament deformation characteristics and its strength. It is known that the processing parameters, especially the graphitization temperature, strongly influence the stiffness and failure strain of the cell ligaments of a graphitic foam. Thus the compressive loading, as discussed above, is

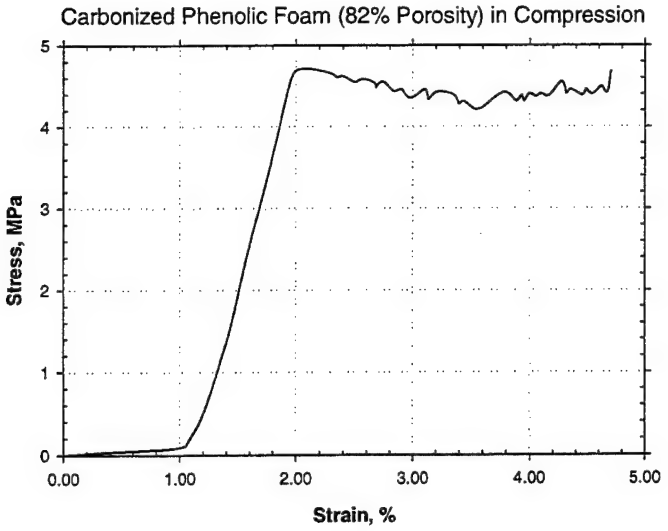

Figure 3. Stress-Strain Curve of a Carbonized Phenolic Open-Cell Foam Subjected to Compression.

not a suitable loading condition to assess the full extent of the ligament deformation mechanism, and the effects of the processing parameters on its failure strain. The tensile loading, in this regard, appears to be a desirable loading condition.

1.1.1 Tensile Loading

Due to high porosity of the material, the tensile coupons prepared from the material could not be directly gripped in the testing frame hydrostatic end grips. Further, in order to apply a uniform displacement on the foam sample subjected to a tensile load, tab materials were bonded to the two ends of the foam sample. Then the tab materials were pin loaded to apply the tensile load to the foam specimen (Figure 4). Specimens of both straightedge and dog-bone-shaped configurations were tested to measure the stress-strain behavior. A diamond saw was used to prepare the straightedge specimens. The dog-bone-shaped specimens were prepared by using an EDM machining tool. A clip extensometer was initially used to measure strain on the specimen surface. However, due to high porosity of

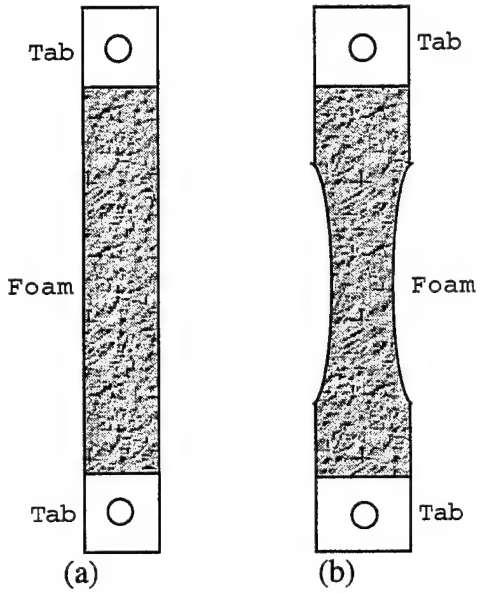

Figure 4. Configuration of the Tensile Foam Specimens: (a) Straightedge Specimen, and (b) Dog-Bone-Shaped Specimen.

the material, a stable contact of the extensometer clip-points on the specimen surface was not obtained. Thus, the strain applied to the specimen was calculated from the machine head displacement, assuming the amount of strain in the bond between the tab and the foam is negligible compared to that of the material in the gage section. The stress-strain curves of the straightedge and dog-bone-shaped specimens are shown in Figures 5 and 6, respectively. The modulus of the material obtained from these two specimen configurations was practically the same. Further, all the specimens tested in these two specimen configurations failed in the gage section. Thus, in view of the simplistic specimen configuration, the straightedge specimen was considered adequate and suitable for the tensile testing for the graphitic foam. The stress-strain curves of a few graphitic foam specimens, using the straightedge specimen configuration, are shown in Figure 7. The modulus and strength of the material are shown in Table 1.

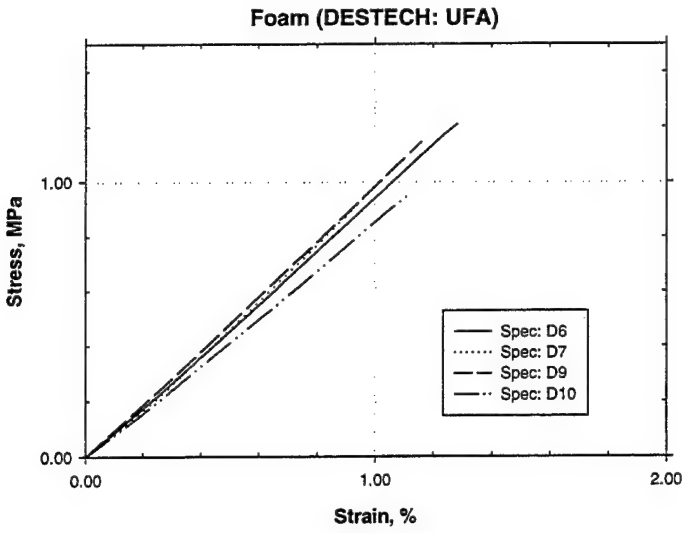

Figure 5. Stress-Strain Curves of Polymeric (Destech: UFA) Foam Straightedge Specimens Subjected to Tensile Loading.

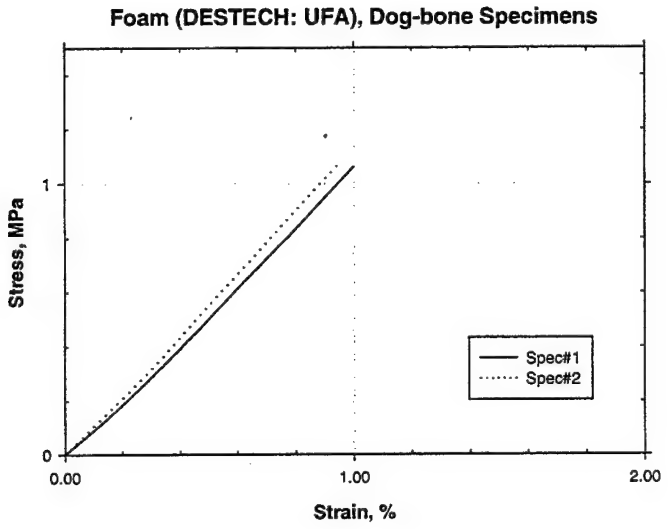

Figure 6. Stress-Strain Curves of Polymeric (Destech: UFA) Foam Dog-Bone-Shaped Specimens Subjected to Tensile Loading.

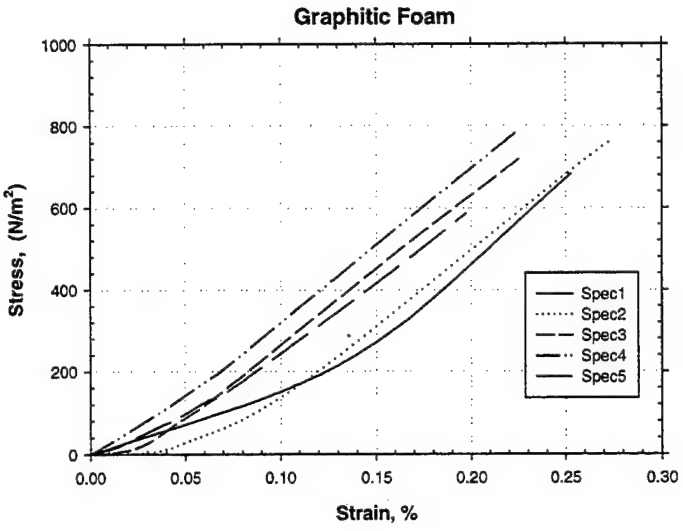

Figure 7. Stress-Strain Curves of Graphitic Foam Specimens in Tensile Loading.

TABLE 1
Modulus and Strength of the Graphitic Foam Samples Tested

Specimen	Width (in)	Thickness (in)	Gage Length (in)	Modulus ksi (GPa)	Strength psi (MPa)
1	0.492	0.252	1.5	48.30 (0.333)	236 (1.63)
2	0.492	0.251	1.7	41.72 (0.288)	227 (1.57)
3	0.492	0.251	1.4	44.03 (0.304)	293 (2.02)

1.1.2 Shear Fixture

The standard shear test, such as the Iosipescu shear test, is not expected to provide reliable shear properties for high-porosity foam. A cylindrical specimen configuration (for example, circular rods) subjected to an axial torsional load is a preferred test for this material to measure its shear properties. A special torsion fixture was designed to measure the shear stiffness and strength of the material, as shown in Figure 8. The twist on the specimen is applied by means of a Worm Gear (60:1 speed reducer) connected to a

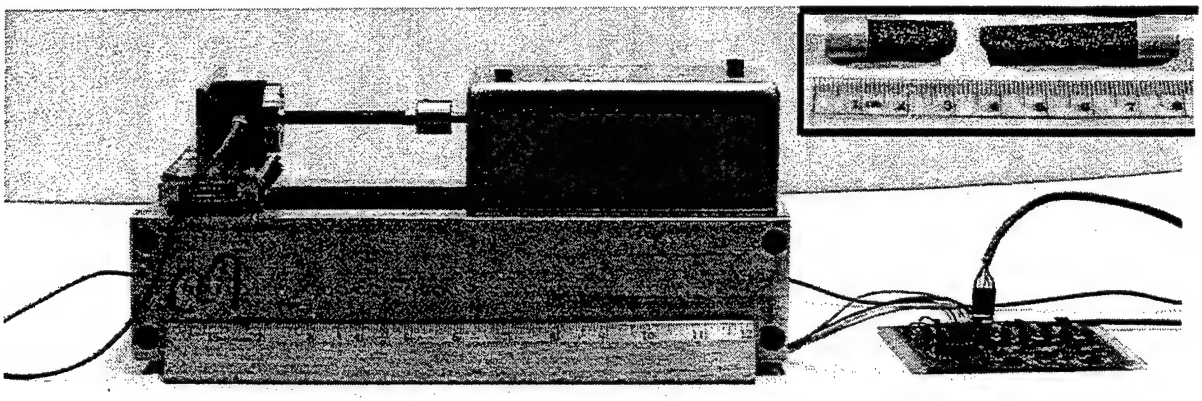

(a)

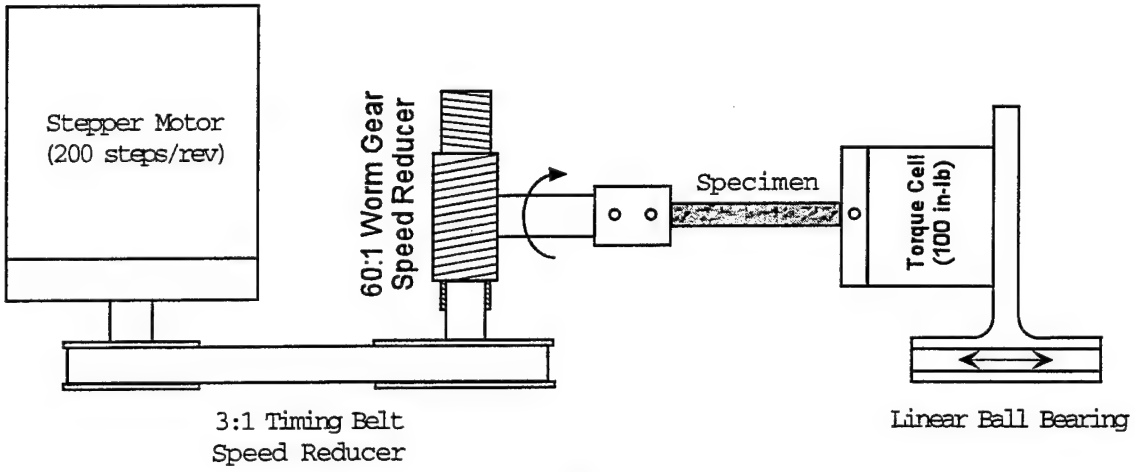

(b)

Figure 8. (a) Shear Test Fixture to Measure Shear Properties (Stiffness and Strength) of Foam Materials, and (b) Schematic Diagram of the Fixture.

stepper motor through a 3:1 timing belt. A 100 in-lb torque cell is used to measure the torque applied on the specimen. The twisting angle is calculated from the step angle of the stepper motor. The two ends of the specimen are secured in the fixture by means of setscrews.

1.2 Summary

The average specific stiffness of the graphitic foam tested above (of density 0.18 gm/cc) is 4.5 ksi/(lb/ft^3), which is about 40 percent higher than that of a polymeric foam used in many structural applications. Because of its superior specific thermal and electrical conductivity over that of a polymeric foam, it is advantageous to use graphitic foam in

applications, such as thermal planes, heat sink, and electronic packaging. Further, the isotropic property of this material makes it an attractive core material (over honeycomb core) in sandwich structures subjected to combined loading. In view of its expected use as a structural material, the tensile test method and a fixture for measuring the shear properties are developed. The tensile test method adapted to a simple specimen configuration is discussed.

2. EXPERIMENTAL AND ANALYTICAL CHARACTERIZATION OF GRAPHITIC FOAMS

2.1 Measurement of Foam Cell Sizes

The standard method of preparing foams in our laboratory for optical microscopy is to vacuum infiltrate with a fluorescently-dyed epoxy potting resin and then polish the plugs flat. The polished plugs are then examined with a Nikon Optiphot FXL microscope in both bright-field and fluorescent illumination. Digital images are obtained using a CCD digital camera. Image analysis of the fluorescent images to measure porosity was straightforward; the open-cell bubbles fill with the fluorescent resin and appear yellow against the black carbon struts. The foams used to develop the cell size technique had average porosity values of 81-82 percent.

Direct measurement of the bubble sizes is not as easy. The usual automated measurements and the ASTM D 2856-70 method are based on the assumption that each bubble can be separated from its neighbor by a cell wall. Then by measuring the observed bubble diameter (d_{meas}) or chord lengths (l_{chord}), the true average diameter can be calculated after accounting for the probabilities of where, within the cell, the measurement is taken:

$$d_{true} = d_{meas}/0.785$$

$$d_{true} = l_{chord}/0.616 = l_{chord}/(0.785)^2$$

In the open-celled carbon foams, the bubble walls have collapsed (at least partially), making it impossible for the computer to separate cells. The human eye can distinguish the individual bubbles using subtle clues which current PC software is incapable of recognizing. To measure the individual bubble diameters on images is tedious and time consuming, but a good estimate of sizes can be obtained by measuring the number of bubbles

in a fixed area (A_{region}). The measured cell diameters can be estimated from the number of cells (n) in a given region:

$$A_{all\ cells} = A_{region} \times \text{Porosity}$$

$$\langle A_{individual\ cell} \rangle = A_{all\ cells}/n = \pi(\langle d_{meas} \rangle/2)^2$$

Square images (selected from a larger one from the regions of interest) all the same size were used. The possible number of bubbles counted will vary depending on which bubbles crossing a boundary are counted. This is shown in the three parts of Figure 9. If all the cells crossing a boundary are counted (Figure 9a), the area of the bubbles is actually higher than estimated; and if none of the bubbles crossing a boundary are counted, (Figure 9b) the area is lower than estimated. The most accurate method would be to count half the bubbles crossing a boundary; arbitrarily we counted the bubbles crossing the left and top boundary (Figure 9c).

The test of this method was the foams in the net-shaped foam project (see AFRL-ML-WP-TR-1999-4026 for results). In that case the regions examined all contained at least several hundred bubbles. It's easy to see that trying to measure the diameters of that many cells would involve a significantly longer amount of time.

2.2 Thermal Characterization of Graphitic Foams

A thermal diffusivity apparatus was moved to its permanent location and a dedicated computer added. Software was updated to allow the measurement of temperatures over time in two modes: the pulse heating method of Parker, et al. *[5]* and the constant heating method of Taylor, et al. *[6]*. Analysis of the data would use the equations below:

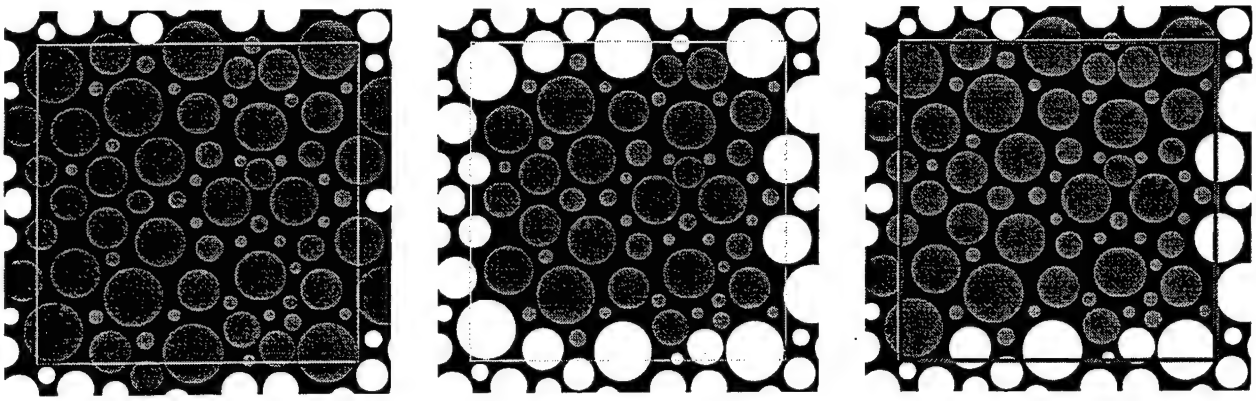

Figure 9. **Schematic Representation of the Possible Number of Bubbles that can be Counted in a Given Area. The area occupied by the bubbles in (a) is larger than would be estimated, in (b) less than estimated, and in (c) approximately the same as estimated.**

$$T = \frac{Q}{\rho C L}\left[1 + 2\sum_{n=1}^{\infty}(-1)^n \exp\left(\frac{-n^2\pi^2}{L^2}\alpha t\right)\right] \qquad \text{Parker - pulse heating}$$

$$T = T_i + \beta_2\left[-\frac{1}{6} + \frac{\alpha t}{L^2} - \frac{2}{\pi^2}\sum\frac{(-1)^n}{n^2}\exp\left(\frac{-n^2\pi^2}{L^2}\alpha t\right)\right] \qquad \text{Taylor - constant heating}$$

where T is temperature on the back of the sample measured as a function of time, α is the sample thermal diffusivity (the goal of this measurement), t is time, L is sample thickness, Q is the heat flux, ρ is density, and C is material heat capacity (lumped together and evaluated as a single curve-fit parameter with L), and β_2 is a constant (evaluated as a curve-fit parameter).

Analyses of theoretical responses are shown in Figures 10 and 11 (note that the time scales in both plots are in seconds). The thermal diffusivities, α, used in this analysis represent values obtained from Oak Ridge National Laboratories on graphitic foams. The thickness of 1 cm was chosen as typical for foam pieces. Note that thicker samples present additional problems with regard to external heat losses, and thinner samples aggravate the

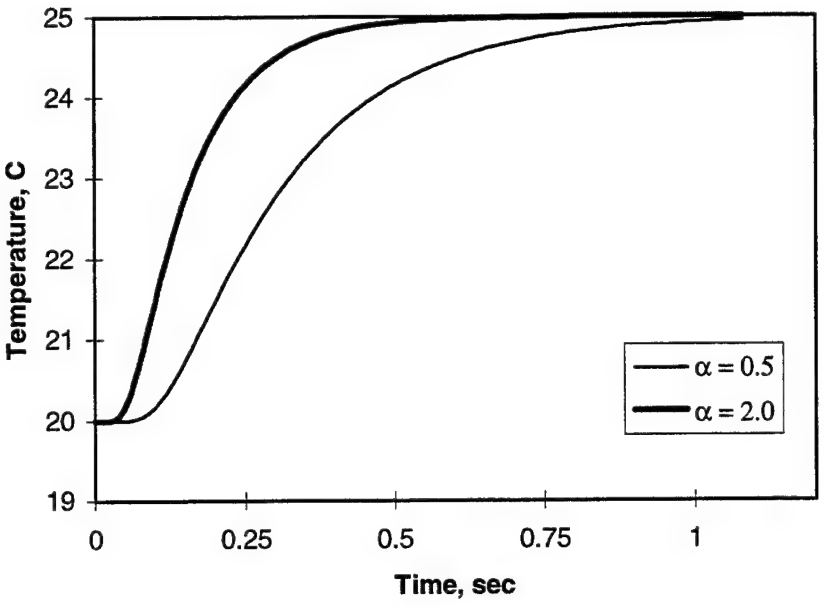

Figure 10. **Theoretical Lines for Pulse Heated Materials 1-cm Thick with $\alpha = 0.5$ cm^2/sec and $\alpha = 2.0$ cm^2/sec.**

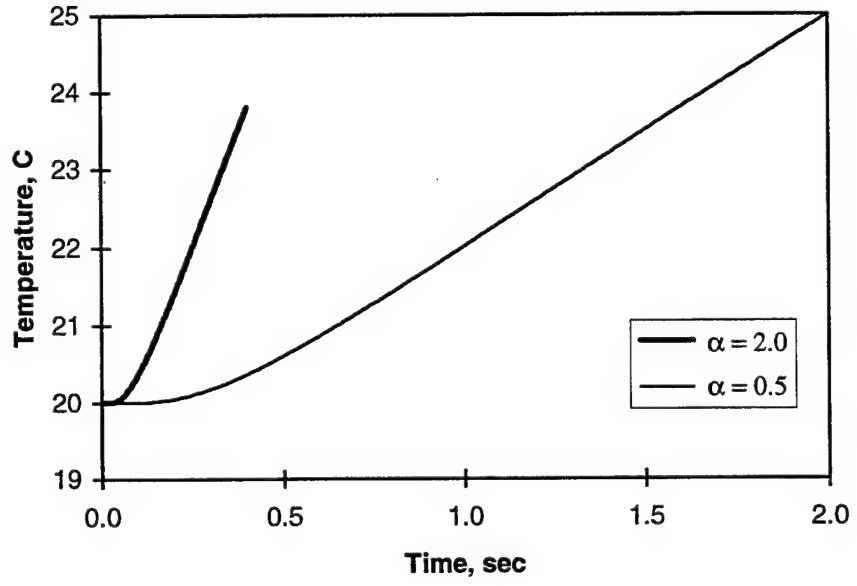

Figure 11. **Theoretical Lines for Constant Heating of Materials 1-cm Thick with $\alpha = 0.5$ cm^2/sec and $\alpha = 2.0$ cm^2/sec.**

problems given below (halving the thickness is equivalent to reducing alpha by a factor of four). Lower alphas make the data collection and analysis easier. The pulse heating technique was ruled out because of the high heat flux required; sufficient heat would have to be added to the sample to raise its temperature several degrees in only a few milliseconds (heating times must be very small relative to heat rise times). The constant heating method allows much lower heat flux – the same total heat to the sample but over seconds rather than milliseconds.

The classic method of analysis is to take the known starting temperature and the slope and intercept of the straight-line region of curve and calculate the thermal diffusivity. This is shown in Figure 12. This method works quite well as long as there is a significant difference between the starting temperature and the straight-line intercept, and there aren't many thermal losses that cause the data to bend over at higher times. The current analysis takes these values as starting points and curve-fits the data using a nonlinear least-squares minimization. The latter is more accurate and is no longer a difficult and time-consuming process with modern PCs.

In practice it was found that taking data at several heat fluxes, giving different heat rises and rise rates, allows the data to be curve fit more effectively. This is shown for a carbon-carbon composite sample in Figure 13. The time interval to be evaluated (while collecting several hundred points) needs to be adjusted dependent on the sample thickness and thermal diffusivity. The graphitic foams need total times of less than a few seconds as shown in Figure 11.

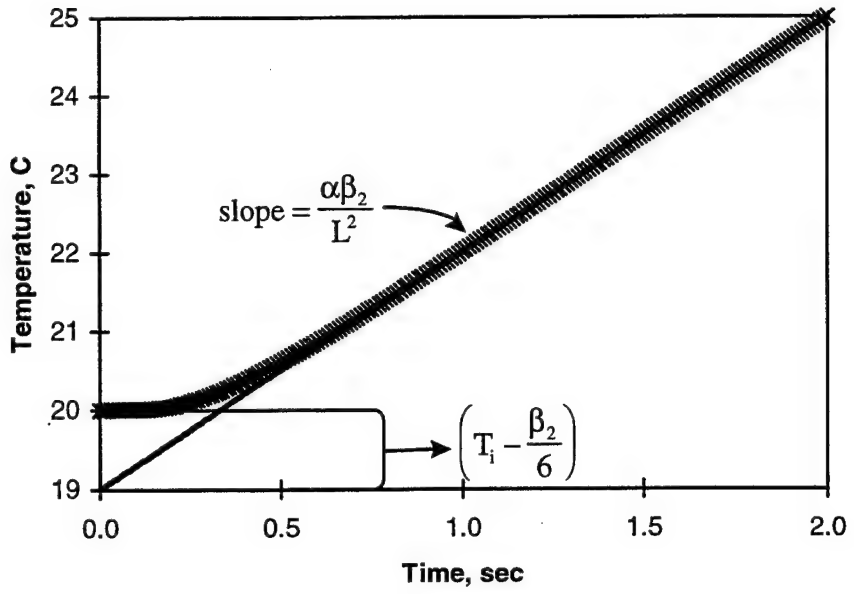

Figure 12. **Theoretical Data Points and Straight-Line Extrapolation for an α = 0.5 cm²/sec Material 1 cm Thick.**

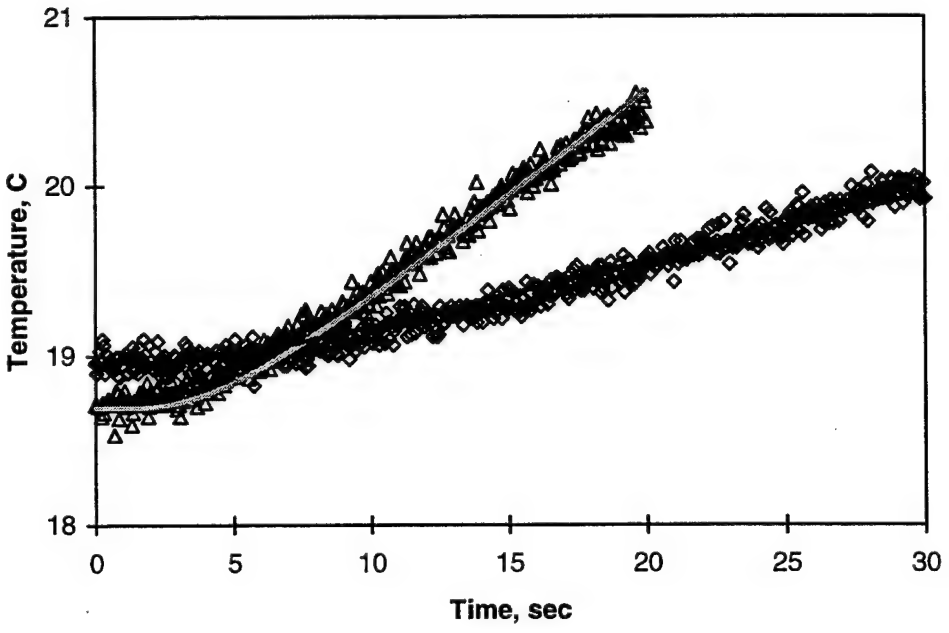

Figure 13. **Temperature Data and Fitted Curves for a Carbon-Carbon Composite with a = 0.0052 cm²/sec at Two Different Heat Flux Levels.**

Attempts to get data on the graphitic foams were inconsistent. This is most likely due to the uneven surface of the foams; sometimes the thermocouple was in contact with the graphite surface and sometimes with air. A larger contact surface, flat-area thermocouple is needed to get the foam data.

2.3 *In Situ* Microscopy and Straining of Foam Samples

Optical microscopy was attempted to observe the deformation of foams, *in situ*, during straining. The limited depth-of-field of the optical microscope requires a well-polished surface which is unavailable in the foams; too much breakage occurs during polishing of an unsupported foam. It was also desired that internal deformations be observed which would not be possible with optical microscopy.

SEMs of the in-house and ORNL foams tested in torsion showed the classic spiral shear failure predicted. The SEM did not reveal any damage in the foam other than the actual failure surface. This is surprising given the rather large deformation (15° twist) prior to failure. The pitch foams may not be as brittle as expected from compression tests.

A straining fixture was rewired to allow its operation in the PSEM microscope. Tests have shown that this device, which uses the thermal expansion of aluminum rods, does not exert sufficient force. To exert a one-percent strain on a foam gage of 3 mm would require aluminum rods to move 30 micrometers or be heated 20°C above ambient over their 2-1/2" lengths. The rods never felt hot so there was insufficient power available to achieve a detectable change in the foam samples.

A different hand-cranked straining stage was used. This Ernst Fuller stage is mountable only on the Joel 840 SEM on the third floor. Initial experiments gave insight to the necessary sample modifications needed to obtain reasonable tests. First the sample gage

length of 10 mm or more had to reduced; narrowing the sides of the foam with a round file produced a dog-bone-shaped sample with a straining gage length of 2-3 mm. Secondly the grip sections of the samples had to be both reinforced mechanically and kept electrically conductive; this was achieved using silver paint.

When these modifications were complete, the sample could be securely mounted without crushing the ends, maintaining electrical contact, and having a gage section small enough to view during straining. The main difficulty of this setup is the requirement of getting Polaroid images versus the digital images available on more modern microscopes. These photographs are both costly and their digitization is time-consuming. However, once that is accomplished the data can be analyzed via image processing software already available.

The initial experiment used the ERG vitreous carbon foams and showed a macroscopic tensile strain of ~1-2 percent (not visible to the eye), while the individual ligaments did not appear to elongate. This is shown in Figure 14 which has the strain measured between two pairs of points widely separated within the gage section of the foam and two points on a single ligament. The overall strain rises monotonically with stress up to the breaking point, while the ligament strain randomly varies about zero a few tenths of a percent. The latter variance in the difference in the final overall strains probably defines the error in the measurements. This result implies the strut angles at the junctures are changing to allow the overall strain. Additional measurements are needed to confirm this as well as measurements on in-house foams.

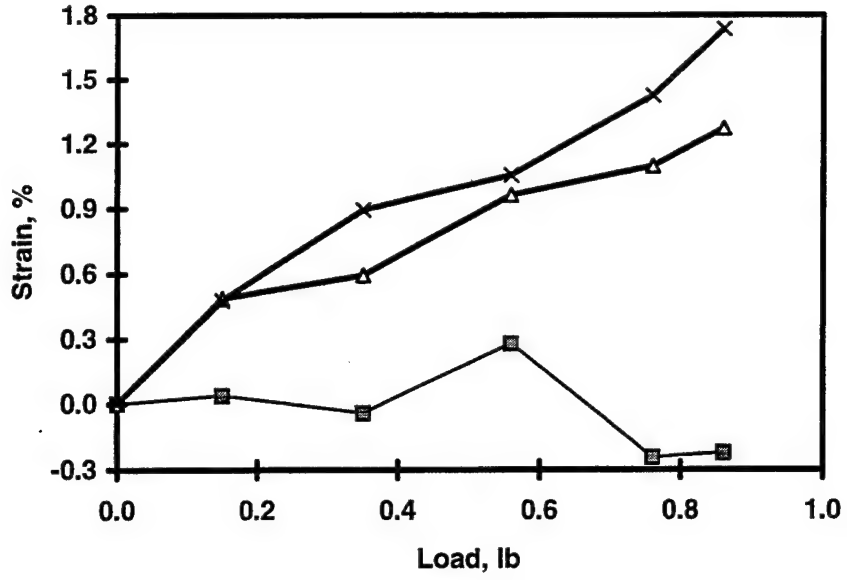

Figure 14. **Strain during Loading of an ERG Vitreous Carbon Foam: Single Ligament (squares) and Two Distances Across the Foam Surface (triangles and crosses).**

2.4 Resurrection of the Control Programs for the Huber 4-Circle X-ray Diffractometer

Both the degree of graphitization and the in-plane crystallite length, L_a, are critical parameters for the prediction of electrical and thermal conductivities of carbon materials. These and other crystalline parameters are also correlated with the mechanical behavior. Since prediction of properties for the pitch-based graphitic foams was an integral part of this delivery order, it became imperative that our ability to measure the crystalline parameters be restored after months of down-time.

The old control programs for the Huber 4-circle diffractometer were written in FORTRAN on a VAX computer running in VMS. Both the computer and operating system were obsolete, and the last failure of the hardware left the diffractometer unable to function. The problems and needs of getting a new program to operate the instrument were:

1. Was a PC sufficient to handle the programming requirements (port old programs to the new machine)?
2. What language would communicate best with the diffractometer interface (make any necessary software changes)?
3. Identify and correct any unknown software problems not inherent in the old programs.
4. Ensure either through software or hardware changes that any additional problems are resolved.

Examination of the old programs established that the amount of communications between the control program and the diffractometer interface could be handled by any of the PCs used back as far as the 8086-based machines. The entire old program was small enough to fit on a single disk and load into 640k of memory. Simple instructions are passed to the interface and data returned and decoded approximately only every 10 seconds. Communication with the diffractometer interface is via a standard RS-232 communications port. An available 486-based machine was chosen since there is no support for computers older than that, but those machines are likely to be around as data collection devices for some time.

Standard FORTRAN was unable to communicate with a communications port. Rather than implement an operating system fix to the problem and to go to a less archaic programming language, it was decided to adapt the program to QuickBasic. While the control programs were being rewritten, they were combined into a single program and made more user-friendly than the older versions. Several specific subroutines that have never been

used by any of the current operators were not translated at this time but could be implemented in the future should their need arise.

The reprogramming required both the changes in how instructions are carried out between FORTRAN and Basic but also an understanding of the machine language instructions sent by the interface and the decoding of the return results. One important aspect of this programming exercise that could benefit any data collection programmer was the understanding that when a program is waiting for a return string, if the operating system is performing any background operations, the program may miss that return string and not proceed to the next instruction. While this background operation problem occurred rarely in Windows 95, it was often enough to be a nuisance. The program was therefore run in MS-DOS 6.22 rather than Windows 95.

During programming, it was noted that the program corrected the diffractometer's motor positions from the encoded positions. The zero positions of the motors were checked and the corrections updated. The interface timing was established as accurate. When data was collected using the new system, several anomalous details revealed themselves. The angles of the diffraction peaks were both not symmetric about the zero point and were higher than they should have been. No test for absolute intensity was possible, but the relative values appeared correct which is sufficient.

These anomalies were fixed in several ways. First the diffractometer hardware had to be aligned by hand in a laborious and time-consuming process. Next the drive commands for the motors have to be checked for accuracy and reproducibility. Software changes were needed to compensate for the encoder errors in three of the four motors. In addition, the detector motor was no longer driving the detector to the correct angles; the

number of pulses per degree had to be changed for both short movements and long movements (corrected in the software). This last problem is a result of wear in the diffractometer and will have to be monitored over time.

The current program allows any operation necessary for aligning the diffractometer, mounting and aligning specimens, manual data collection, and automated data collection of Bragg scans and azimuthal scans. One feature added to the program was the ability to change a scan request if the instructions originally given were outside of the hardware limits; in the past such requests terminated the program. Other features added included the ability to mix the type of scans programmed at any one time, and standard scans can be requested without having to input all the drive commands each time.

Data collection has resumed on heat-treated fibers and measurements of the degree of graphitization of the foams from MLBC, ORNL, and WVU. The results are shown in Table 2 along with the measurements of thermal conductivity made at ORNL on these materials. High degrees of graphitization and large crystallite size are both needed to get good thermal conductivities. It can be seen in the table that the ORNL had the highest specific thermal conductivity as well as the highest degree of graphitization and L_a. It should be noted that while thermal conductivity increases with L_a, this parameter also correlates with poor compression strength in carbon fibers *[7]*.

TABLE 2
Crystalline Parameters and Externally Measured Thermal Properties of Several Graphitized Foam Samples

Foam Origin	k (W/m-K)	k/ρ (W/m-K/g/cm^3)	g_p (%)	L_a (nm)
ORNL	73.2	128.8	96	16.7
MLBC	16.9	71.3	97	11.5
WVU	13.9	49.6	63	17.1

k = thermal conductivity
k/ρ = specific thermal conductivity
g_p = degree of graphitization
L_a = in-plane graphitic crystallite size

3. REFERENCES

1. Anderson, Heather J., Kristen M. Kearns, & David P. Anderson. (1997). Microcellular Graphitic Foams. *Proc. 23rd Biennial Conference on Carbon,*

2. Kearns, Kristen M., & David P. Anderson. (1997). Microcellular Graphitic Foam Processing. *Proc. 11th International Conference on Composite Materials.*

3. Anderson, David P., Kristen M. Kearns, Cindy Tucci, & Gerry Mestemaker. (1998). The Cellular Structure of Net Shaped Pitch-Based Microcellular Carbon-Foams. *Proc. 43rd International SAMPE Symp.*

4. Anderson, Heather J., Kristen M. Kearns, & David P. Anderson. (1998). Microcellular Pitch-Based Carbon Foam Blown with Helium Gas. *Proc. 43rd International SAMPE Symposium and Exhibition.*

5. Parker, W. J., R. J. Jenkins, C. P. Butler, & G. L. Abbott. (1961). Flash Method of Determining Thermal Diffusivity, Heat Capacity, and Thermal Conductivity. *J. Appl. Phys.* 32 (1679).

6. Taylor, R. E., T. R. Goerz, & J. V. Beck. (1996). Automatic Non-destructive Brake Tester for Thermal Diffusivity/Conductivity of Aircraft Brake Disks. *Operations Manual for Properties Research Laboratory*, West Lafayette, IN.

7. Anderson, D. P. & A. S. Crasto. (1996). A Microstructural Study of Carbon Fibers for Thermal Management and Space Applications. *Proc. of Space Technology and Applications International Forum (STAIF-96)* (869).